

Model Development for Oxygen Diffusion through Petroleum Contaminated Soils.

Umeda, Uchendu, and Ehirim, Emmanuel

Department of Chemical/ Petrochemical Engineering

Rivers State University, Portharcourt, Nigeria.

Corresponding Author: Umeda, Uchendu

ABSTRACT: The aim of this study was to develop a Mathematical model that will predict oxygen concentration at 100cm depth, obtained from oxygen diffusion for bioremediation of petroleum contaminated soils at above mentioned depth. A mathematical model in two dimensional flow(x and z) was developed from basic conservative principle and it was solved numerically to obtain the final solution. MATLAB 8.1a version (R 2013) was used to simulate the entire process. Results obtained from the model for oxygen concentration at 100cm depth followed the same trend with the experimental results. The results from the model were compared with experimental results and both showed a good fit. Therefore, the developed model can be used for the prediction of Oxygen concentration for bioremediation of petroleum contaminated soils at 100cm depth.

Keyword: Mathematical Model; Oxygen Diffusion and

Date of Submission: 02-06-2019

Date of acceptance: 17-06-2019

I. INTRODUCTION

Bioremediation is a process that offers the possibilities to destroy or render various contaminants harmless, using natural biological activities (Vidali, 2001). Bioremediation involves three principal approaches namely, natural attenuation, bio-stimulation and bio-augmentation (Chikere et al., 2009a). For effective bioremediation to take place in the soil, there must be sufficient soil nutrient and oxygen concentration, to enhance the activities of microorganism (Umeda et al., 2017). Nutrients are easily assimilated by soil microorganisms in soil pollution with crude oil, thus reducing the nutrient reserves (Rahman et al., 2002). Petroleum biodegradation is highly dependent on environmental conditions and on the chemical structure of the pollutant compounds (Swannell et al., 1996; Aldrett et al., 1997). The rates of degradation and the quality of hydrocarbon eliminated also depend on the type and amount of hydrocarbon present at the contaminant site (Del Arco and de Franca, 2001). Components that are low in molecular weight such as the aliphatic hydrocarbons tend to be degraded first, leaving behind the much larger molecules (aromatic hydrocarbon) which take much longer to break down. The lighter carbon components of the crude oil are also less viscous and can easily degrade and become volatile when acted upon by weather and environmental elements. This trend indicates the presence of biodegradation by microbial bacteria who cannot break down the larger oil compounds left after the initial phases of degradation (Ezra et al., 2000). Hydrocarbons from crude oil are substrates for microorganisms, hence, when an accidental oil spill occurs, the number of hydrocarbon degrading microorganisms in the ecosystem increases. The speed and efficiency of bioremediation of a soil contaminated with petroleum and petroleum products depend on the number of hydrocarbon-degrading microorganisms in the soil. The most important factors for population growth are temperature, oxygen, pH, content of nitrogen and phosphorus, hydrocarbon class and their effective concentration. Also, the degree and rate of biodegradation are influenced by the type of soil in which the process occurs (Van hmm et al., 2003).

DEVELOPMENT OF MATHEMATICAL MODEL

Mathematical Model for oxygen diffusion through petroleum contaminated soils at 100cm depth in two dimensional flow (x and z) was developed from basic conservative principle as shown below.

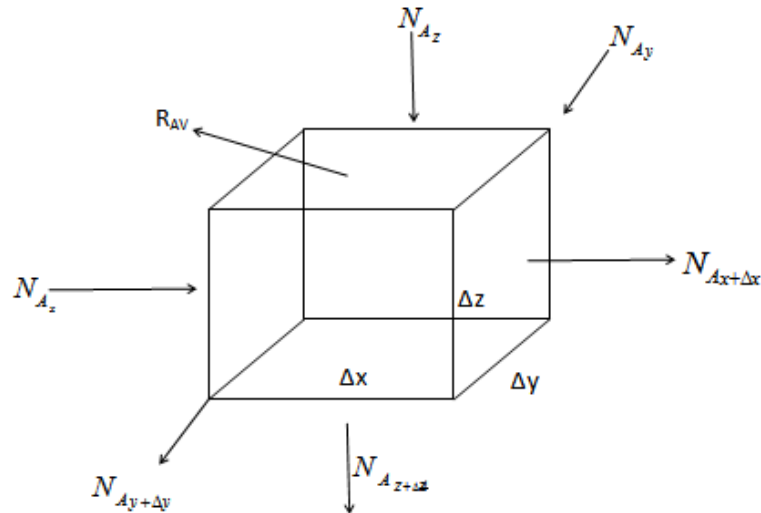


Figure 1. Schematic Diagram for the Hypothetical Control Volume Representation of Soil Sample

Considering the conservation of species A, including production of A by chemical reaction within the volume. The general relation for mass balance of species A for the control volume is stated as

$$\left[\begin{array}{l} \text{Net rate of mass} \\ \text{efflux of A from} \\ \text{control volume} \end{array} \right] + \left[\begin{array}{l} \text{Net rate of} \\ \text{Acceleration of A} \\ \text{within control volume} \end{array} \right] - \left[\begin{array}{l} \text{Rate of chemical} \\ \text{production of A within} \\ \text{the control volume} \end{array} \right] = 0 \quad (1)$$

Defining individual terms in equation (1) and deriving from basic conservative principle, we obtain the following.

The net rate of mass efflux from the control volume could be evaluated by considering the mass transferred across control surfaces. Hence, the mass of A transferred across the area

$$\Delta y \Delta z \text{ at } x \text{ will be } \rho_A V_{Ax} \Delta y \Delta z / x$$

$$\text{That is, } n_{Ax} \Delta y \Delta z / x.$$

The net rate of mass efflux of component A will be

$$\text{In the x-direction: } n_{Ax} \Delta y \Delta z / x + \Delta x - n_{Ax} \Delta y \Delta z / x$$

$$\text{In the y - direction: } n_{Ay} \Delta y \Delta z / y + \Delta y - n_{Ay} \Delta y \Delta z / y$$

$$\text{and in the z - direction: } n_{Az} \Delta x \Delta y / z + \Delta z - n_{Az} \Delta x \Delta y / z$$

$$\text{Rate of accumulation of volume A with control} = \frac{\partial \rho_A}{\partial t} \Delta x \Delta y \Delta z$$

$$\text{Rate of reaction by chemical reaction} = r_A \Delta x \Delta y \Delta z$$

Substituting each terms in equation (1), we obtain

$$n_{Ax} \Delta y \Delta z / x + \Delta x - n_{Ax} \Delta y \Delta z / x + n_{Ay} \Delta x \Delta z / y + \Delta y - n_{Ay} \Delta x \Delta z / y + n_{Az} \Delta x \Delta y / z + \Delta z - n_{Az} \Delta x \Delta y / z +$$

$$\frac{\partial \rho_A}{\partial t} \Delta x \Delta y \Delta z - r_A \Delta x \Delta y \Delta z = 0 \quad (2)$$

Dividing through by the volume $\Delta x \Delta y \Delta z$, and cancelling terms, we have

$$\frac{n_{Ax} / x + \Delta x - n_{Ax} / x}{\Delta x} + \frac{n_{Ay} / y + \Delta y - n_{Ay} / y}{\Delta y} + \frac{n_{Az} / z + \Delta z - n_{Az} / z}{\Delta z} + \frac{\partial \rho_A}{\partial t} - \rho_A = 0 \quad (3)$$

Evaluated in the limit as $\rho_A \Delta x \Delta y \Delta z$ approaches zero, this yields

$$\frac{\partial \eta_{Ax}}{\partial x} + \frac{\partial \eta_{Ay}}{\partial y} + \frac{\partial \eta_{Az}}{\partial z} + \frac{\partial \rho_A}{\partial t} - r_A = 0 \quad (4)$$

Eq. (4) is the equation of continuity of component A. As η_{Ax} , η_{Ay} and η_{Az} are the rectangular components of the mass flux vector, η_{Ax} ; equation (4) may be written

$$\nabla n_A + \frac{\partial \rho_A}{\partial t} - r_A = 0 \quad (5)$$

A similar equation of continuity for component B in the same manner. The differential equation are

$$\frac{\partial n_{Bx}}{\partial x} + \frac{\partial n_{By}}{\partial y} + \frac{\partial n_{Bz}}{\partial z} + \frac{\partial \rho_B}{\partial t} - r_B = 0 \quad (6)$$

and $\nabla \cdot n_B + \frac{\partial \rho_B}{\partial t} - r_B = 0 \quad (7)$

Adding equations (5) and (7), we obtain:

$$\nabla \cdot (n_A + n_B) + \frac{\partial (\rho_A + \rho_B)}{\partial t} - (r_A + r_B) = 0 \quad (8)$$

But

$$n_A + n_B = \rho_A V_A + \rho_B V_B = \rho V$$

$$\rho_A V_B = \rho$$

Substituting these relation with eq. (8)

$$\nabla \cdot \rho V + \frac{\partial \rho}{\partial t} - (r_A + r_B) = 0 \quad (9)$$

Eq. (9) represents the continuity equation for the mixture.

Writing equation (9) in substantial derivative

$$\frac{D\rho}{Dt} + \rho \nabla \cdot V = 0$$

$$\frac{\rho D W_A}{Dt} + \nabla \cdot \rho_A - r_A = 0 \quad (10)$$

Molar equivalent of eq. (5) and (7) are

For component A

$$\nabla N_A + \frac{\partial C_A}{\partial t} - R_A = 0 \quad (11)$$

For component B

$$\nabla N_B + \frac{\partial C_B}{\partial t} - R_B = 0 \quad (12)$$

and for mixture (adding equation (11) and (12)) we have

$$\nabla (N_A + N_B) + \frac{\partial (C_A + C_B)}{\partial t} - (R_A + R_B) = 0 \quad (13)$$

For a binary mixture

$$N_A + N_B = C_A V_A + C_B V_B = CV$$

and $C_A + C_B = C$



$$\nabla \cdot CV + \frac{\partial C}{\partial t} - (R_A + R_B) = 0 \quad (14)$$

Recall,

$$\begin{aligned} N_A &= -CD_{rB} \nabla \cdot y_A + y_A (N_A + N_B) \\ &= -CD_{AB} \left(\frac{\partial y_A}{\partial x} + \frac{\partial y_A}{\partial y} + \frac{\partial y_A}{\partial z} \right) + y_A (N_A + N_B) \end{aligned}$$

OR

$$N_A = -CD_{AB}\nabla y_A + C_A V \tag{15}$$

Substituting eq. (15) into eq. (11), we obtain

$$-\nabla \cdot CD_{AB}\nabla y_A + \nabla \cdot C_A V + \frac{\partial C_A}{\partial t} - R_A = 0 \tag{16}$$

$$-CD_{AB}\nabla^2 y_A + \nabla C_A V + \frac{\partial C_A}{\partial t} - R_A = 0$$

Eq. (16) describes concentration problems within a diffusing system. This equation is relatively unwieldy. These equations can be simplified by making restrictive assumptions.

Assumptions:

1. If the density ρ and D_{AB} are constant

$$-CD_{AB}\nabla^2 y_A + V \nabla C_A + \frac{\partial C_A}{\partial t} - R_A = 0$$

$$-D_{AB}\nabla^2 C_A + V \cdot \nabla C_A + \frac{\partial C_A}{\partial t} - R_A = 0$$

$$-D_{AB}\nabla^2 \rho_A + \rho_A \nabla \cdot V + V \cdot \nabla \rho_A + \frac{\partial \rho_A}{\partial t} - r_A = 0$$

Dividing each term by the molar weight of component A and rearranging we obtain

$$V \cdot \nabla C_A + \frac{\partial C_A}{\partial t} = D_{AB} \nabla^2 C_A \pm R_A \tag{17}$$

$$V_x \frac{\partial C_A}{\partial x} + V_y \frac{\partial C_A}{\partial y} + V_z \frac{\partial C_A}{\partial z} + \frac{\partial C_A}{\partial t} = D_{AB} \left\{ \frac{\partial^2 C_A}{\partial x^2} + \frac{\partial^2 C_A}{\partial y^2} + \frac{\partial^2 C_A}{\partial z^2} \right\} \pm R \tag{18}$$

Where

The solution to equation (18) was solved numerically

$$R = \frac{1}{Y} \frac{\mu_m SX}{K_s + S}$$

using the *Finite Different Approximation* (FDA) in the explicit scheme. Thus, resolving the resulting partial differential equation numerically, we obtain the following:

The initial and boundary conditions are as follows

At $t = 0, z \geq 0$ and $x \geq 0: C = 0$

At $t > 0, z = 0$ and $x = 0: C = C_0$

At $t > 0, z > 0$ and $x > 0: C = C_\infty$

$$\frac{\partial C}{\partial t} = \frac{C_{i,j}^{k+1} - C_{i,j}^k}{\Delta t} \tag{19}$$

$$\frac{\partial C}{\partial z} = \frac{C_{i,j+1}^k - C_{i,j-1}^k}{2\Delta z} \tag{20}$$

$$\frac{\partial^2 C}{\partial x^2} = \frac{C_{i+1,j}^k - 2C_{i,j}^k + C_{i-1,j}^k}{\Delta x^2} \tag{21}$$

$$\frac{\partial^2 C}{\partial y^2} = \frac{C_{i+1,j}^k - 2C_{i,j}^k + C_{i-1,j}^k}{\Delta y^2} \tag{22}$$

$$\frac{\partial^2 C}{\partial z^2} = \frac{C_{i,j+1}^k - 2C_{i,j}^k + C_{i,j-1}^k}{\Delta z^2} \tag{23}$$

The diffusion of oxygen in y direction is minimal because of the driving force in the z direction, so the diffusion of oxygen in the y direction is insignificant.

Substituting equations (19) and (23) into (18) yields:

$$\frac{C_{i,j}^{k+1} - C_{i,j}^k}{\Delta t} = D \left[\frac{C_{i+1,j}^k - 2C_{i,j}^k + C_{i-1,j}^k}{\Delta x^2} + \frac{C_{i,j+1}^k - 2C_{i,j}^k + C_{i,j-1}^k}{\Delta z^2} \right] - v \left[\frac{C_{i,j+1}^k - C_{i,j-1}^k}{2\Delta z} \right] - R_{i,j}^k \quad (24)$$

For uniform grids $\Delta x = \Delta z$, therefore, equation (6) becomes

$$C_{i,j}^{k+1} - C_{i,j}^k = \frac{\Delta t D}{\Delta x^2} (C_{i+1,j}^k - 2C_{i,j}^k + C_{i-1,j}^k + C_{i,j+1}^k - 2C_{i,j}^k + C_{i,j-1}^k) - \frac{\Delta t v}{2\Delta z} (C_{i,j+1}^k - C_{i,j-1}^k) - \Delta t R_{i,j}^k \quad (25)$$

Collection of like terms

$$C_{i,j}^{k+1} = \frac{\Delta t D}{\Delta x^2} (C_{i-1,j}^k + C_{i+1,j}^k) + \left(1 - 4 \frac{\Delta t D}{\Delta x^2} \right) C_{i,j}^k + \left(\frac{\Delta t D}{\Delta x^2} + \frac{\Delta t v}{2\Delta z} \right) C_{i,j-1}^k + \left(\frac{\Delta t D}{\Delta x^2} - \frac{\Delta t v}{2\Delta z} \right) C_{i,j+1}^k - \Delta t R_{i,j}^k \quad (26)$$

Also, the reaction term $R_{i,j}^k = \frac{1}{Y} \frac{U_m S X}{K_s + S}$ and $S = C$.

Hence,
$$R_{i,j}^k = \frac{1}{Y} \frac{U_m X C_{i,j}^k}{K_s + C_{i,j}^k} \quad (27)$$

Substituting equation (7) into (6) gives

$$C_{i,j}^{k+1} = \frac{\Delta t D}{\Delta x^2} (C_{i-1,j}^k + C_{i+1,j}^k) + \left(1 - 4 \frac{\Delta t D}{\Delta x^2} \right) C_{i,j}^k + \left(\frac{\Delta t D}{\Delta x^2} + \frac{\Delta t v}{2\Delta z} \right) C_{i,j-1}^k + \left(\frac{\Delta t D}{\Delta x^2} - \frac{\Delta t v}{2\Delta z} \right) C_{i,j+1}^k - \Delta t \frac{1}{Y} \frac{U_m X C_{i,j}^k}{K_s + C_{i,j}^k} \quad (28)$$

Equation (28) is the numerical solution in two dimensional flow (x and z) to the model in the explicit scheme. Where C- Initial Oxygen Concentration, D-Diffusion coefficient of oxygen in the soil, Y- Yield conversion constant, U_m - Maximum specific growth rate, K_s - Substrate Saturation constant, Z- Distance, t - Time. Equation (28) is the model for prediction of oxygen concentration with time and depth along the reactor.

Calculation Algorithm

The algorithm for implementation of the model solution is shown in Figure 2 as follows.

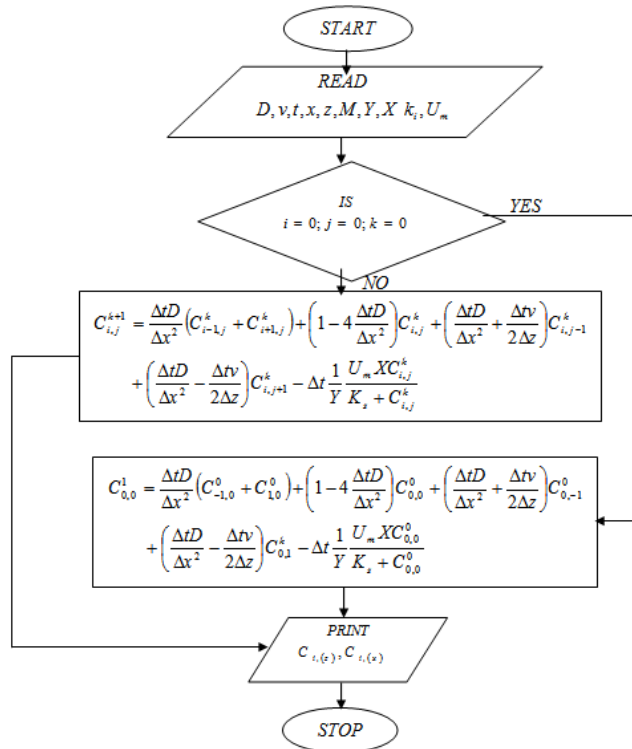


Figure 2: Flow Algorithm for Oxygen Diffusion and Carbon Dioxide Productio

II. RESULTS AND DISCUSSION

Surface Plot of Oxygen Diffusion in Sandy Soils

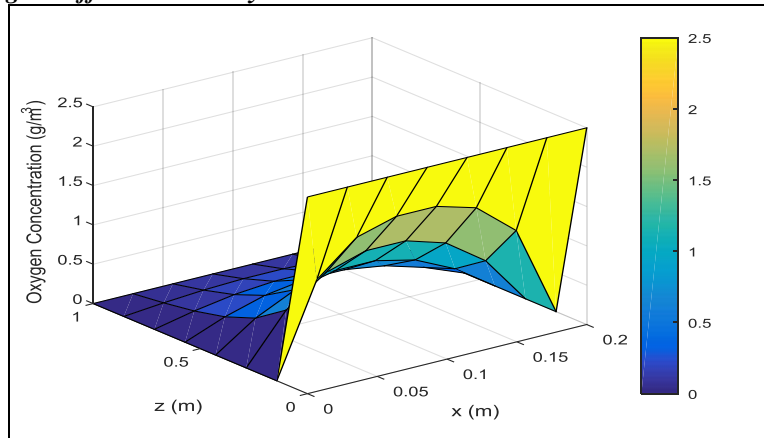


Figure 3: Diffusion of Oxygen in Sandy Soil (2 Weeks)

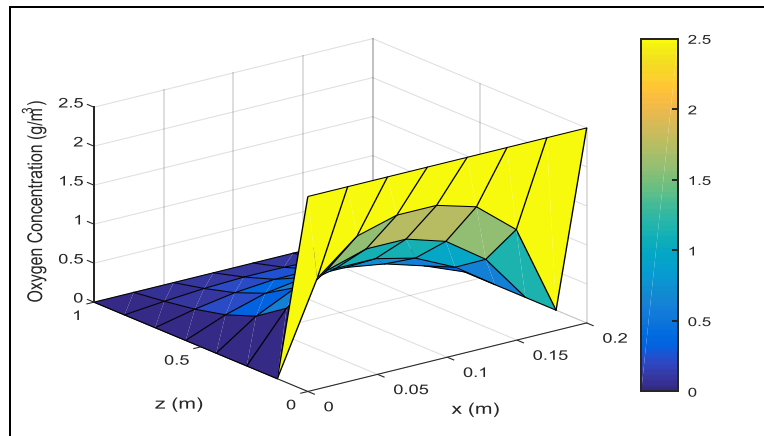


Figure 4: Diffusion of Oxygen in Sandy Soil (4 Weeks)

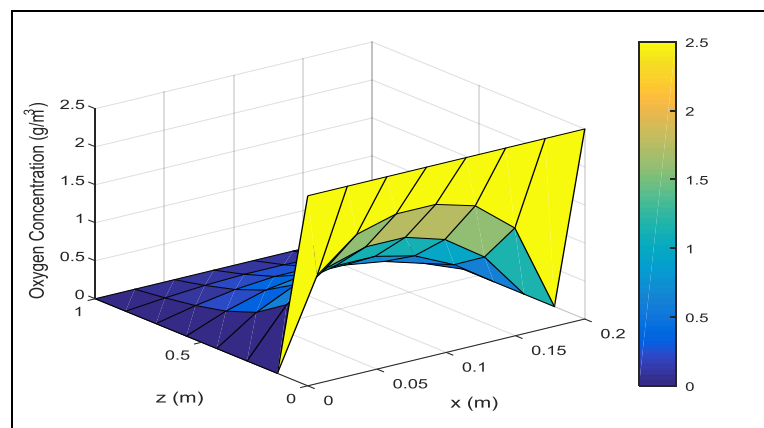


Figure 5: Diffusion of Oxygen in Sandy Soil (6 Weeks)

Surface Plot of Oxygen Diffusion in Sandy Loam Soils

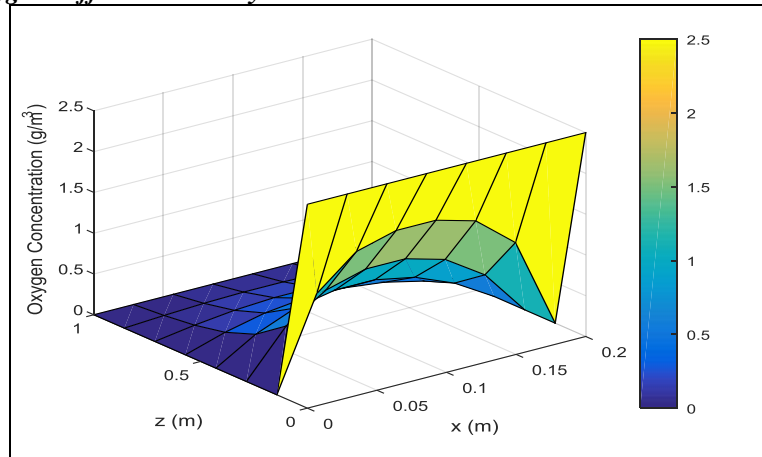


Figure 6: Diffusion of Oxygen in Sandy Loam Soil(2 Weeks)

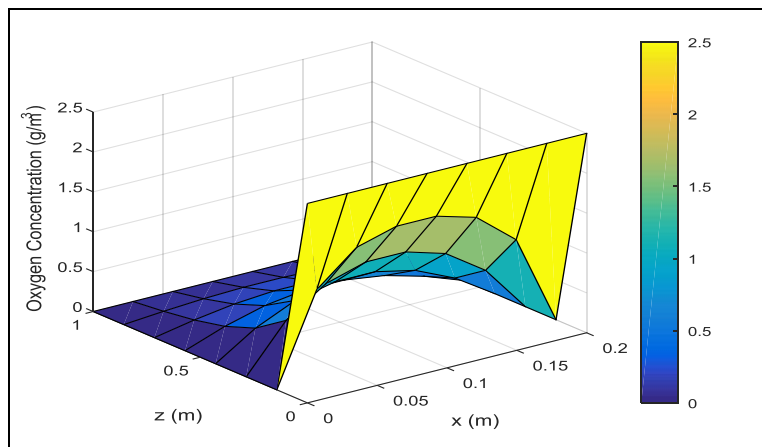


Figure 7: Diffusion of Oxygen in Sandy Loam Soil(4 Weeks)

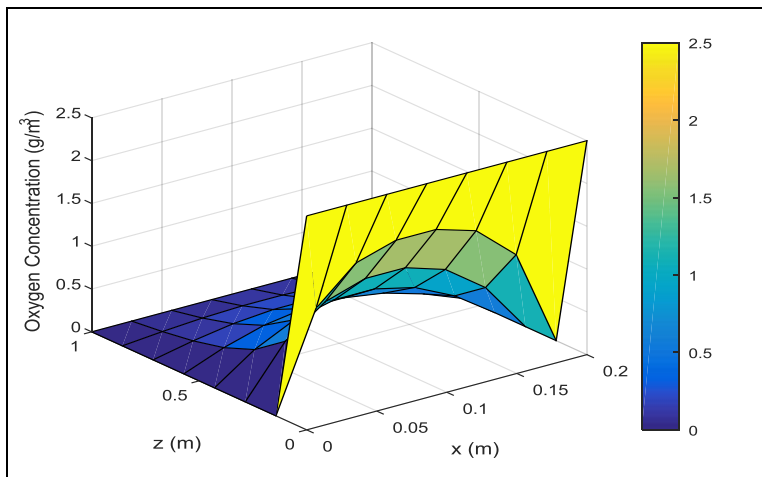


Figure 8: Diffusion of Oxygen in Sandy Loam Soil (6 Weeks)

Surface Plot of Oxygen Diffusion in Clay Soils

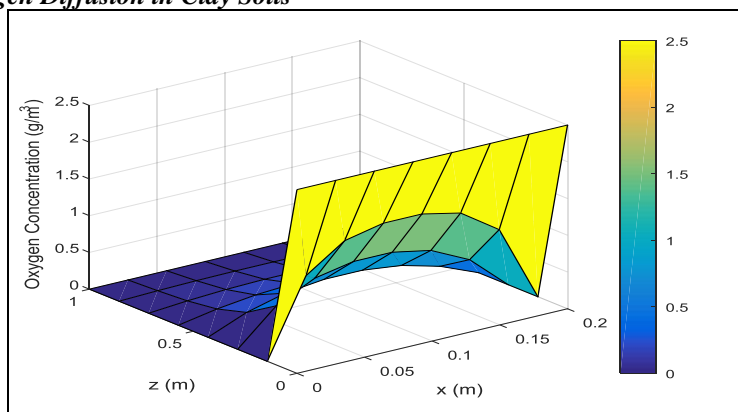


Figure 9: Diffusion of Oxygen in Clay Soil (2 Weeks)

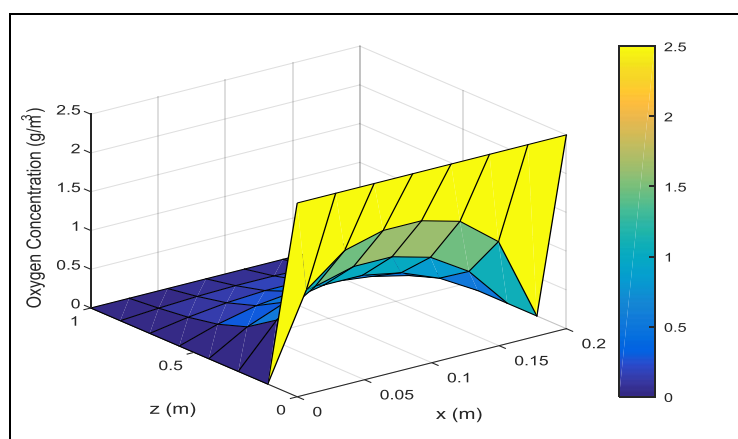


Figure 10: Diffusion of Oxygen in Clay Soil (4 Weeks)

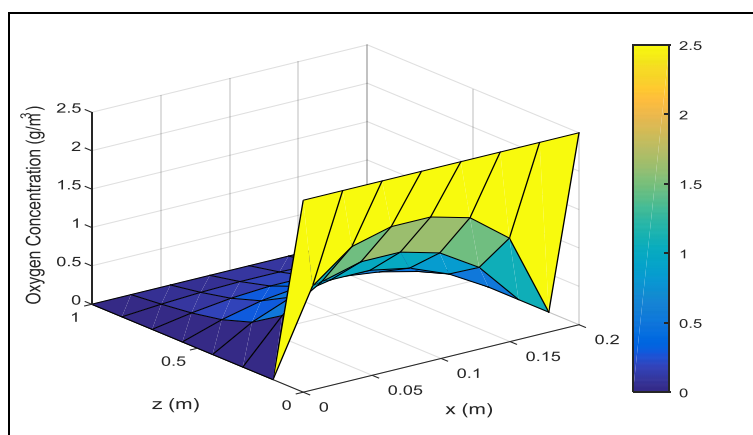


Figure 11: Diffusion of Oxygen in Clay Soil (6 Weeks)

Figures 3 – 11 (obtained from MATLAB simulations) show surface plots of oxygen concentration diffusing into x and z direction in Sandy soil, Sandy loam and Clay soil. The plot shows that the concentration was constant at the initial point of deposition with very high concentration which diffused into x and z direction. The different colour indicated in the graph showed the different in concentration of the oxygen as it diffused in x and z direction. The graph indicated that the concentration of oxygen diffusion decreased with depth and time in x and z direction. This implied that the result followed the same trend with the experimental results. Also, it showed that the developed model predicted the experimental results reasonably well. Oxygen diffusion rate of the soils were obtained from the graphs of the developed model as $7.5 \times 10^{-04} \text{ mg l}^{-1} \text{ h}^{-1}$, $8.3 \times 10^{-04} \text{ mg l}^{-1} \text{ h}^{-1}$ and $2 \times 10^{-03} \text{ mg l}^{-1} \text{ h}^{-1}$ for Sandy, Sandy loam and Clay soil respectively. These values were obtained by calculating the area under the representative curves.

COMPARISON BETWEEN EXPERIMENTAL AND MODEL PREDICTIVE DATA FOR OXYGEN CONCENTRATION.

The basis of the comparison of the experimental and model data was to show the fitness of the data at all data point and the trend obtained from the experimental and predictive model results.

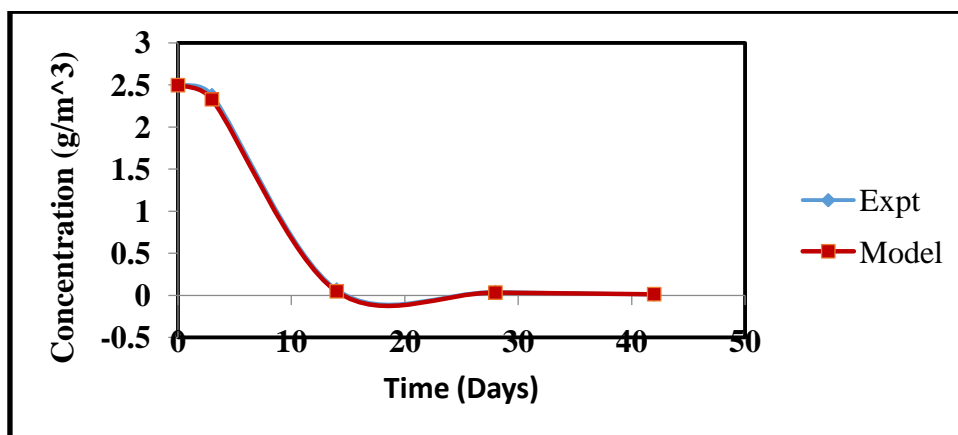


Figure 12: Comparison between Experimental and Model Predictive Data for Sandy Soil

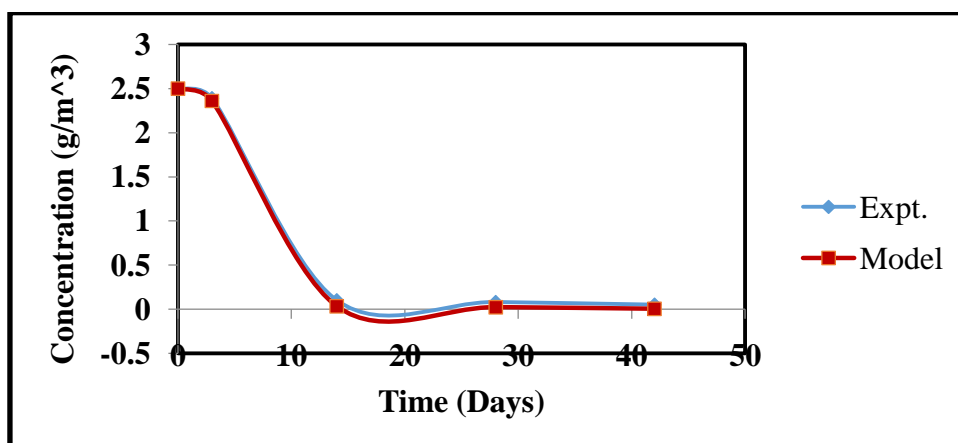


Figure 13: Comparison between Experimental and Model Predictive Data for Sandy Loam Soil

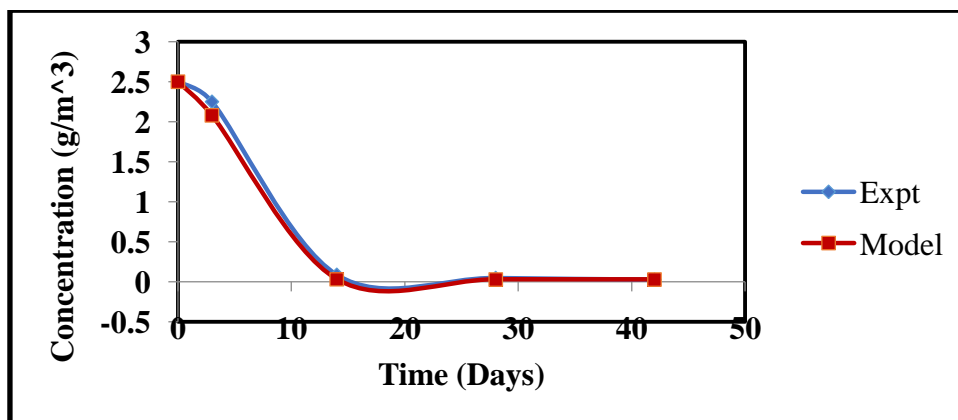


Figure 14: Comparison between Experimental and Model Predictive Data for Clay Soil

Figures 12- 14, indicated that the predictive model gives very good fit of experimental Data at all Data point with an error of 0.01%, 0.04% and 0.02% for Sandy Soils, Sandy Loam Soil and Clay Soil respectively. Also, it showed that the results of the experimental and predictive model followed the same trend.

COMPARISON OF OXYGEN DIFFUSION IN SANDY SOILS, SANDY LOAM AND CLAY SOILS

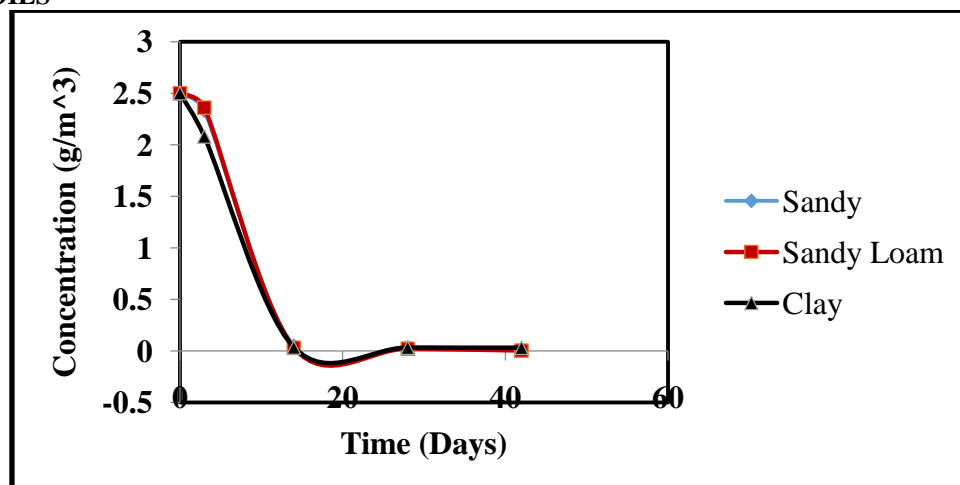


Figure 15: Comparison of Results of Oxygen Diffusion in the Soils.

Figure 15 shows the graph of oxygen diffusion in Sandy soils, Sandy loam and Clay soils. Comparison of Oxygen diffusion in Sandy soils, Sandy loam and Clay soil reveal that the diffusion of Oxygen is highly appreciable in Clay Soil compared to Sandy and Sandy loam soils. This may be as a result of the particle size of the soils, surface area, and porosity of the soils.

III. CONCLUSION

In line with the results obtained from this study, it is important to state that the developed mathematical model can be used for the prediction of Oxygen concentration for bioremediation of petroleum contaminated soils at 100cm depth.

REFERENCES

- [1]. Aldrett, I., Bonner, S., Mills, J.S., Antenneth, M.A. & Stephen, R.L.(1997). Microbial degradation of crude oil in Marine environments tested in ask experiment. *Water Research*, 31,2840-2848
- [2]. Chikere, C.B., Okpokwasili G.C., & Ichiakkor, O. (2009a). Characterisation of hydrocarbon utilizing bacteria in tropical marine sediments. *African Journal of Biotechnology*, 11,2541-2544
- [3]. Del Arco, J.P. & De Franca, F.P. (2001). Influence of oil contamination level on hydrocarbon biodegradation in sandy sediment. *Environmental Pollution*, 110, 515-519
- [4]. Ezra, S., Feinstein, S., Pelly, I., Banman, D. & Miloslavsky, I. (2000).Weathering of fuel oil spill on the east Mediterranean coast, Ashdod, Isreal.*Organic Geochemistry*.3, 1733-1741.
- [5]. Rahman, K.S.M., Thahira-Rahman, J., Lakshamapermamsamy, P.& Banat, I. M. (2002).Towards efficient crude oil degradation by a mixed bacterial consortium.*Bio-resources Technology*, 85, 257 – 261.
- [6]. Swannel, R.P.J.,Lee, K. & Mc Donagh, M. (1996). Field evaluation of marine oil spill bioremediation. *Microbiological Review*, 60, 343-365.
- [7]. Umeda, U., Puyate, Y.T., Dagde, K.K. & Ehirim, E.O. (2017). Effect of oxygen diffusion on Total Petroleum Hydrocarbon in Petroleum contaminated soils. *International Journal of Engineering and Modern Technology*,3, 18-24
- [8]. Van Hamme, J.D., Singh, A. & Ward, O.P. (2003). Recent advances in petroleum microbiology. *Microbial Molecular Biology Review*, 67, 503-549.
- [9]. Valadi, M. (2001). Bioremediation. An overview, *Appli. Chem*, 73, 1163 -1172

Umeda, Uchendu. "Model Development for Oxygen Diffusion through Petroleum Contaminated Soils." *IOSR Journal of Engineering (IOSRJEN)*, vol. 09, no. 06, 2019, pp. 54-63.